Lightning protection of a multi-circuit HV-MV overhead line

Lightning Protection of a Multi-Circuit HV-MV Overhead Line

A. Borghetti*, G. M. Ferraz^, F. Napolitano*, Carlo Alberto Nucci*, A. Piantini°, Fabio Tossani*,

* Department of Electrical, Electronic and Information Engineering, DEI, University of Bologna, Italy

^ High Voltage Equipment, HVEX, Itajubá, Brazil

° Institute of Energy and Environment, University of Sao Paulo, Brazil

Corresponding author. E-mail address: fabio.tossani@unibo.it

Abstract

This paper deals with the assessment of the lightning performance of a medium voltage (MV) power line sharing the same poles of a high voltage (HV) line. We focus on the case of a 15-kV line with compact configuration that is supported by the concrete poles of a 69-kV or a 138-kV transmission line. Due to the taller HV pylons and conductors, the number of direct events to the multi-circuit line is higher than for a MV line alone. The presence of the HV conductors and of the overhead ground wire reduces the amplitudes of the induced overvoltages in the MV conductors due to indirect lightning events. For the considered configurations, with a compact MV line, the number of flashovers per year expected in the double-circuit line due to both direct and indirect flashes is lower than in a MV line alone. It is shown that such a number depends mainly on the line withstand voltage, on the grounding resistance and on the number of surge arresters. The dependence is quantitatively discussed in the paper. The analysis of the overvoltages transferred on the LV side of the distribution transformers is also performed.

Keywords: multi-circuit overhead lines; lightning performance; induced voltages; surge arresters.

1. Introduction

In some areas characterized by low availability either of land or ways of right for building overhead lines, it is convenient to install a medium voltage (MV) distribution line on the same pylons or poles holding a high voltage (HV) transmission line. The resulting multi-voltage overhead line configuration poses peculiar issues with respect to both the electromagnetic coupling between the conductors of the MV and HV lines, as analyzed in [1], and the voltages across the insulators due to direct strikes [2].

The presence of grounded wires in the HV line reduces the voltage peak amplitudes induced in the MV line by the indirect lightning events. However, due to the taller poles the incidence of direct events on the hybrid line is much larger than the one expected for a MV line alone, which justifies a specific analysis for this double circuit configuration.

The analysis presented in [3] focuses on the lightning performance assessment of the MV line. In this paper the analysis is enlarged in order to evaluate the induced voltages transferred to the low voltage (LV) side of the MV/LV transformers connected to the line. The analysis is aimed at defining a set of guidelines so to differentiate the protecting means in the various feeders and to include the installation of protections only where it is effective and necessary to achieve the desired level of expected number of failures.

This paper presents:

i) time domain simulations of the lightning-induced overvoltages due to nearby strokes and the overvoltages due to direct strikes; these are accomplished by using the LIOV-

EMTP-RV software [4,5], which has been adapted to the specific characteristics of the case under investigation;

ii) the statistical assessment of the lightning performance of the double-circuit line due to both indirect and direct events, by using the Monte Carlo procedure presented in [6], [7]. The statistical assessment is presented for different values of the grounding resistance and different distances between surge arresters along the MV line. Moreover, the influence of flashovers in the HV insulators on the lightning performance of the MV line is analyzed too.

The structure of the paper is the following. Section II describes the geometry of the line and the LIOV-EMTP-RV model. Section III presents some time domain results for both indirect and direct events aimed at providing some insight into the lightning response of the multi-circuit configuration. Section IV presents the lightning performance assessment for the different considered cases. Section V concludes the paper.

2. Geometry of the Line and LIOV-EMTP Models

This paper considers the two overhead line structures shown in Figure 1: a) 69-kV line, b) 138-kV line. In both cases the MV line (15 kV insulation class) has a compact structure, i.e. insulated phase wires (without shield) with reduced distances secured by periodical spacers suspended by an upper unenergized wire called messenger. The MV line is located below the HV conductors, 7 m above ground in a) and 9 m in b).

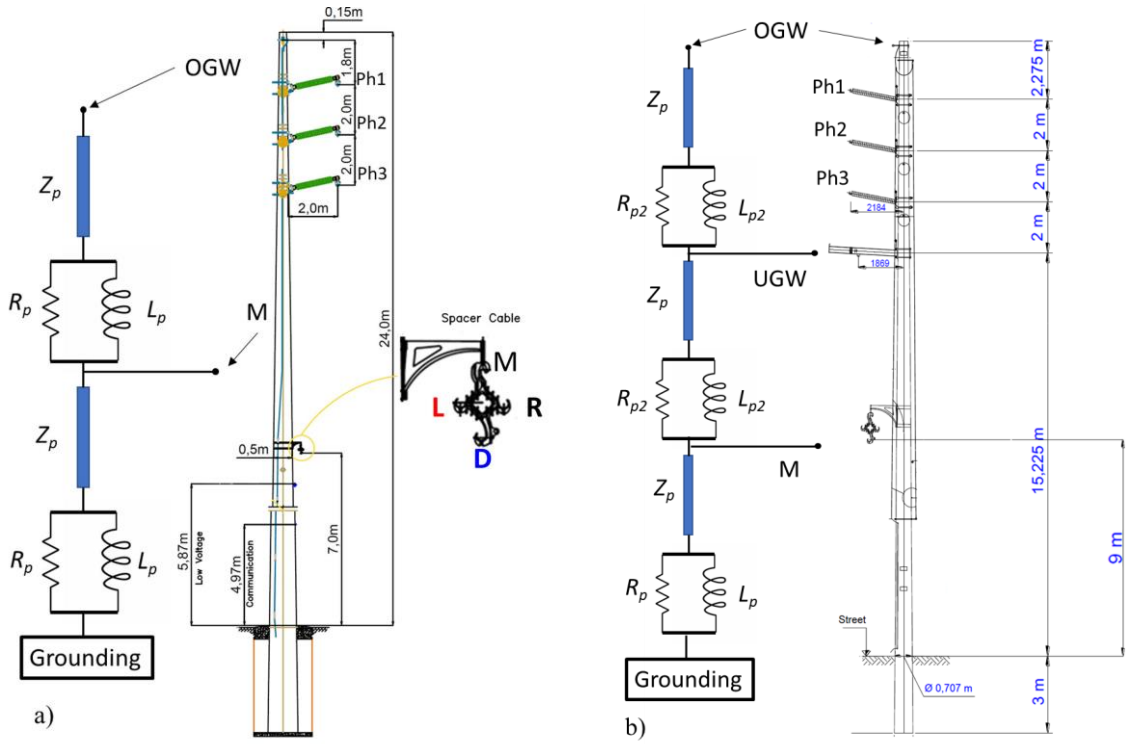

Figure 1. Geometry and EMTP model of the considered concrete poles of the double-circuit line: a) 69-kV transmission line, b) 138-kV transmission line.

On the top of both structures there is an overhead ground wire (OGW) grounded at every pole. Moreover, the 138-kV line has an underbuilt ground wire (UGW) located 2 m below the lowest phase conductor, grounded at each pole, that reduces the back flashover rate, as described in [8].

Between two consecutive poles of the HV line, in the middle of each span, there is a lower MV pole, having the function of sustaining the compact MV line only. The span distances between the 69-kV line poles and the 138-kV line poles are 70 m and 80 m, respectively. In all the simulations we assume the ground conductivity σ_g = 1 mS/m.

The value of the pole surge impedance is assumed equal to Z_p = 200 Ω according to the experimental data presented in [9]. As shown in Figure 1a, the pole of the 69-kV configuration is split in two sections, one between the heights of the OGW and of the messenger (point M) and the other between point M and ground. The 138-kV pole has

been split in three sections (Figure 1b): between OGW and UGW (5 m high), between UGW and M (5 m), and M and ground (10 m). This is not in perfect agreement with the dimensions shown in Fig. 1; the reason why the length of each pole section has been rounded to integer multiples of 5 m is that such an approximation, which does not affect the accuracy of the results, makes the implementation of the EMTP model more straighforward.

The values of the damping resistance and inductance of the model shown in Figure 1 are estimated according to the method proposed in [10]. Their values are R_p = 33 Ω and L_p = 5.33 μH, R_{p2} = 16.6 Ω and L_{p2} = 2.66 μH.

The effect of the soil ionization is represented by using Weck's formula [11]. The ratio between the value of the grounding resistance considering soil ionization R_w and the dc grounding resistance in absence of ionization R_g is given by

$$\frac{R_w}{R_g} = \frac{1}{\sqrt{1 + I / I_g}} \tag{1}$$

where

$$I_g = \frac{E_0}{2\pi\sigma_g R_g^{\,2}} \tag{2}$$

I is the current flowing in the grounding system and E_0 is the soil breakdown gradient, taken equal to 400 kV/m.

In the statistical analysis reported in Section IV, the insulation breakdown is modeled by means of the disruptive effect (DE) criterion [12]. According to this criterion, the following integral is considered

$$D = \int_{t_0}^{t} \left[|v(t)| - V_0 \right]^k dt \tag{3}$$

where $v(t)$ is the voltage across the insulator, V_0 is the minimum voltage to be exceeded before any breakdown process can start, k is a dimensionless factor, and t_0 is the time at which $|v(t)|$ becomes greater than V_0. A flashover occurs if integral D becomes greater than a constant value DE. The parameters V_0, DE and k for both HV and MV insulators are reported in Table 1.

Table 1. Parameters assumed for the disruptive effect model

Voltage class (kV)	***CFO* (kV)**	**DE model parameters**		
		V_0 (kV)	k	DE (kVμs)
15 (covered)		246	1	134
15 (bare)		160	1	100
69	740	570	1.36	9180
138	670	516	1.36	8020

Assuming the critical flashover overvoltage (*CFO*) value of the HV lines as known, the parameters of the DE-model of the HV insulators are estimated by applying the following expressions [8], [13], [14], where *CFO* is in kV:

$$V_0 = 0.77 CFO \tag{4}$$

$$DE = 1.15\, CFO^{1.36} \tag{5}$$

The parameters of the DE-model for the MV line are inferred by using the voltage vs time-to-breakdown curve (*V-t* curve) provided by the experimental data obtained for the 15-kV spacer and the bare conductors. For the covered conductors, the contribution of the XLPE coverage (with thickness ranging from 2.3 to 3.3 mm) is estimated by adding 100 kV to the voltage peak amplitudes of the abovementioned experimental curve for bare conductors [15]. The estimated *V-t* curve is in reasonable agreement with the experimental data for covered conductors presented in [16].

Figure 2 shows the *V-t* experimental data along with the *V-t* curve described by the following function:

$$V(t) = A + B / t^C \tag{6}$$

where *A*, *B* and *C* are determined by a least-squares fitting procedure.

Assuming $k = 1$ and a 1.2 / 50 μs impulse voltage, the parameters of the DE model of Table 1 are obtained by a nonlinear least-square minimization of the differences between the times to breakdown given by the fitted function (6) and the ones given by the DE model (3). Figure 2 also shows the comparison between the *V-t* curve obtained by the experimental data and the corresponding curve obtained by the DE model with the parameters of Table 1.

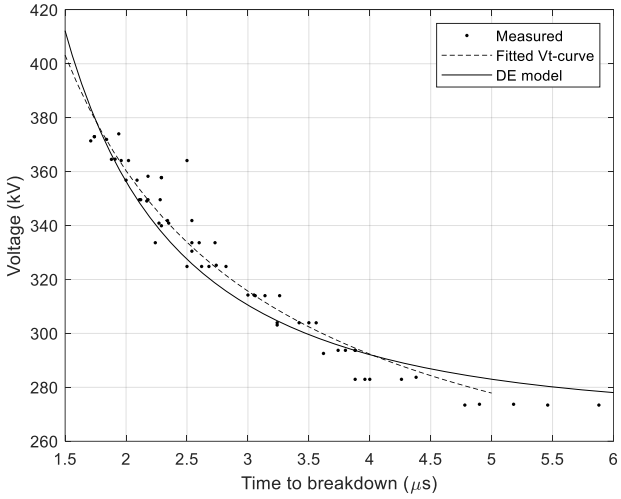

Figure 2. Comparison between the V-t curve fitted by using experimental data with XLPE covering and the one predicted by the DE model.

Table 2 shows the voltage-current characteristic of the surge arresters (SAs) installed in the MV line.

Table 2. Characteristic of the SAs in the MV line

Current (A)	Voltage (V)
0.001	21200
1500	27000
3000	29500
5000	31500
10000	36000
20000	41500
40000	53000

We also consider the presence of MV/LV transformers and LV lines supported by the same poles of the 15-kV and 69-kV lines, as shown in Figure 1a). The LV line is composed by four insulated conductors (three phases, denoted as *l, d, r* in the following figures, and the neutral one, denoted as *n*) located at 5.85 m above the ground. The transformers are simulated in EMTP by means of the high frequency model presented in [17].

For the calculation of the induced voltages due to indirect strokes we assume the shielding effect of nearby buildings as negligible. This effect has, however, a significant influence on the lightning performance of overhead lines in urban areas as shown in [18], [19] .

We also neglect the effect of the lightning electromagnetic pulse in the calculation of the overvoltages due to direct strikes, as it is a minor contribution, as shown in [20].

In all the simulations presented in this paper, the effect of surge propagation losses is neglected. The impact of surge propagation losses on the amplitude and shape of lightning induced overvoltage in distribution lines is discussed in e.g., [21], [22].

3. Time Domain Analysis

This section presents the transient response of the double-circuit line (69-kV configuration) to the external incident electromagnetic field originated by a nearby

lightning return stroke, and to a direct strike. In these time domain simulations, the presence of SAs along the line is not considered.

The MV conductors are denoted as messenger (M), left phase conductor (L), down phase conductor (D), and right phase conductor (R).

The line is 1400 m long and is matched at both terminations with the line surge impedance matrix. With respect to a system of *x*-*y* coordinates centered in the middle point of the line, with *x* axis parallel to the line, the stroke location coordinates are x = 35 m, y = 50 m. The return stroke velocity is assumed to be 1.5×10^8 m/s; the Transmission Line (TL) return stroke model is assumed for the simulations. The channel-base current has a peak amplitude of 12 kA and a maximum time-derivative of 40 kA/μs, which are typical median values of subsequent return strokes [23]. The current waveform is represented by using the sum of two Heidler functions [24] with the following parameters [25]: I_{01} = 10.7 kA, τ_{11} = 0.25 μs, τ_{21} = 2.5 μs, n_1 = 2, I_{02} = 6.5 kA, τ_{12} = 2.1 μs, τ_{22} = 230 μs, n_2 = 2.

In Figure 3, the overvoltages induced by the subsequent stroke in the MV conductors at the line center of the double-circuit configuration are shown for the case of R_g = 20 Ω. The overvoltages are calculated between the wires and the undisturbed far earth, assumed at zero potential. Figure 4 shows the corresponding voltages induced in the conductors of the MV line alone, i.e., without the presence of the HV circuit.

The comparison between Figure 3 and Figure 4 shows that the overvoltage peak amplitudes are slightly lower in the MV phases of the double-circuit configuration. Figure 3 shows that the voltage in conductor M of the double-circuit line is higher than in the MV line alone (Figure 4). This is due to the induced voltages in the OGW at 24 m above ground that produces a potential rise in the common grounding system. This is the main

reason for the lower voltage across the MV insulators (i.e., the voltage difference between the phase conductors and the messenger) in the double-circuit line respect to the MV line alone.

The oscillations of the voltages shown in Figure 3 are due to the reflections at the OGW groundings.

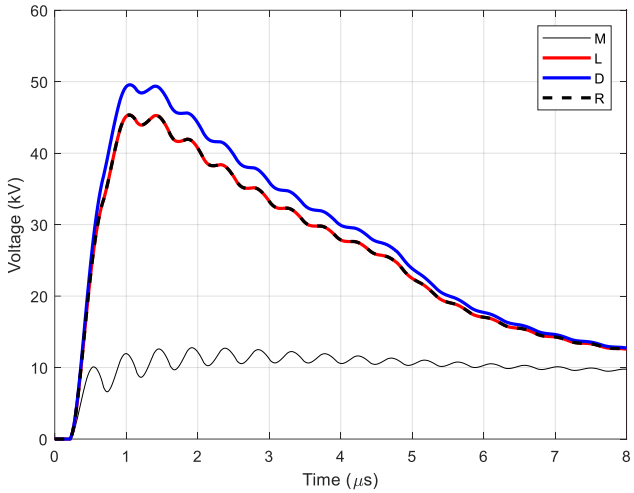

Figure 3. Voltage induced by a subsequent stroke in the MV conductors of the 69-kV line. R_g = 20 Ω.

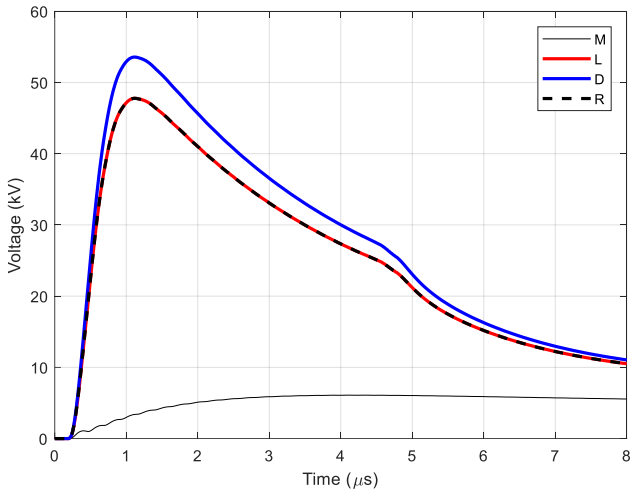

Figure 4. Voltage induced by a subsequent stroke in the MV conductors in absence of HV line. R_g=20 Ω.

We now consider a channel-base current with a peak value of 31 kA and a maximum time-derivative of 26 kA/μs, assumed as typical of a first negative return stroke,

represented by the Cigré current function [11]. Figure 5 shows the overvoltages in the 69-kV line due to a direct strike to OGW in the middle of the line. Figure 6 shows the overvoltages for the 138-kV configuration where also the UGW is present. The value of the grounding resistance is R_g = 40 Ω and the soil ionization is taken into account.

The presence of the UGW reduces the voltage between the phases and the grounded wires (OGW and UGW). The UGW, therefore, reduces the back-flashover rate of the HV phase conductors, especially concerning the farthest phase from the OGW (phase 3). The comparison between Figure 5b and Figure 6b shows that also the voltage between conductors M and D is slightly lower in the 138-kV configuration than in the 69-kV one.

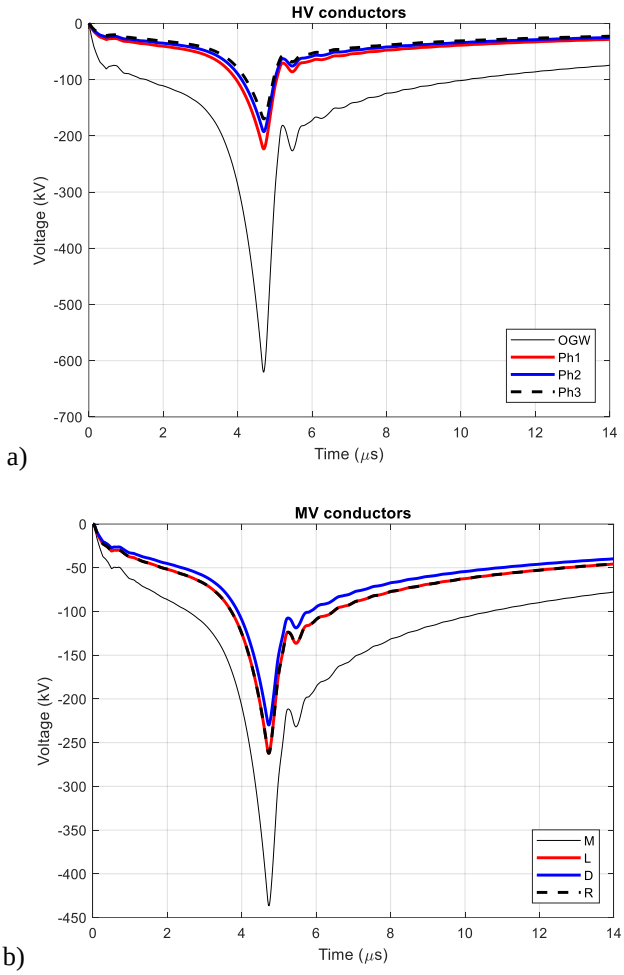

Figure 5. Overvoltages in the 69-kV line due to a direct strike to OGW in the middle of the line: a) HV conductors; b) MV conductors. R_g=40 Ω.

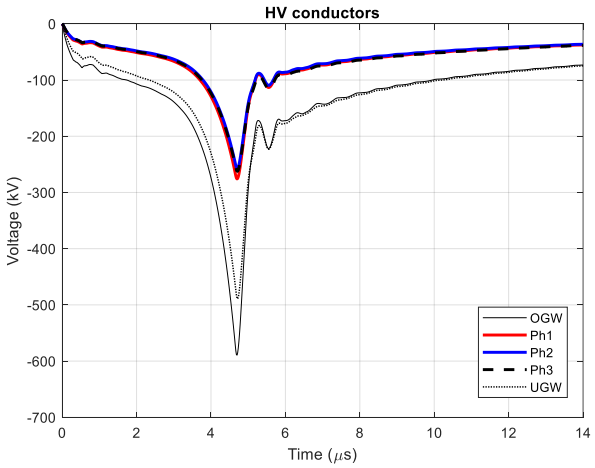

a)

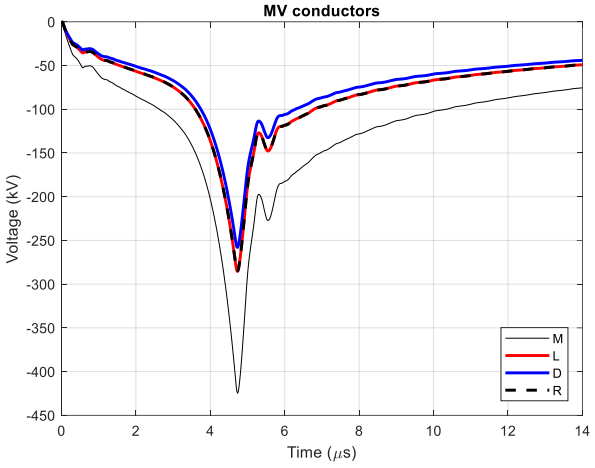

b)

Figure 6. Overvoltages in the 138-kV line due to a direct strike to OGW in the middle of the line: a) HV conductors; b) MV conductors. R_g=40 Ω.

We have repeated the simulations of Figure 3 and Figure 4 by disregarding the soil ionization and by using two different grounding models: a) a lumped grounding resistance; b) four counterpoises represented by using the model given in [26]. The obtained results are very similar to those shown in Figure 3 and Figure 4 due to the low value of the ground conductivity.

The analysis of the induced voltages in the LV line has been carried out by considering the triple-circuit configuration shown in Figure 7, in which the presence of a LV line is considered in addition to the others. A couple of MV/LV transformers are mounted on two of the poles. Three LV lines are connected to the LV side of the transformers, with

length equal to 10, 15 and 20 m. The grounding resistance is 15 Ω for the medium and low voltage poles and 20 Ω for the high voltage towers.

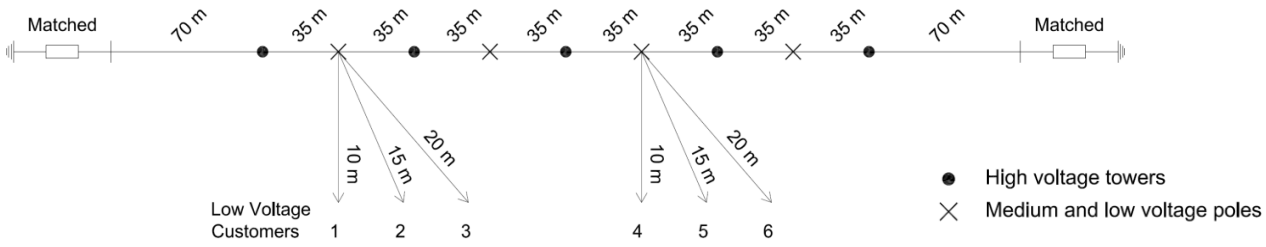

Figure 7. Top view of the network topology, with location of towers, poles and low voltage customers

Surge arresters are installed at the MV side of the transformers and surge protective devices (SPD) are installed between each phase and the neutral at the end of the LV lines. The neutral is grounded at both ends by a 15 Ω grounding resistance.

The LV-SPD characteristic is reported in Table 3.

Table 3. Characteristic of the LV-SPDs.

Current (A)	Residual voltage (V)
0.001	470
0.1	580
10	650
100	770
1000	950
10000	1200

Figure 8 shows the overvoltages at the two transformers LV terminals due to a nearby negative first stroke. The return stroke is represented by means of a Heidler function with the following parameters: $I_0 = 29.3$ kA, $\tau_1 = 1.44$ μs, $\tau_2 = 91.8$ μs, $n = 2$. The stroke location is 75 m far from the line center. Although the phase-to-neutral voltages are limited by the SPDs, the overvoltages on the neutral conductor at the LV side of each transformer customers assume very high values.

In the considered case, the far end of the neutral wire can reach voltages larger than 7 kV, as shown in Figure 9, and this could endanger the insulation of the LV equipment in case of incomplete equipotential bonding.

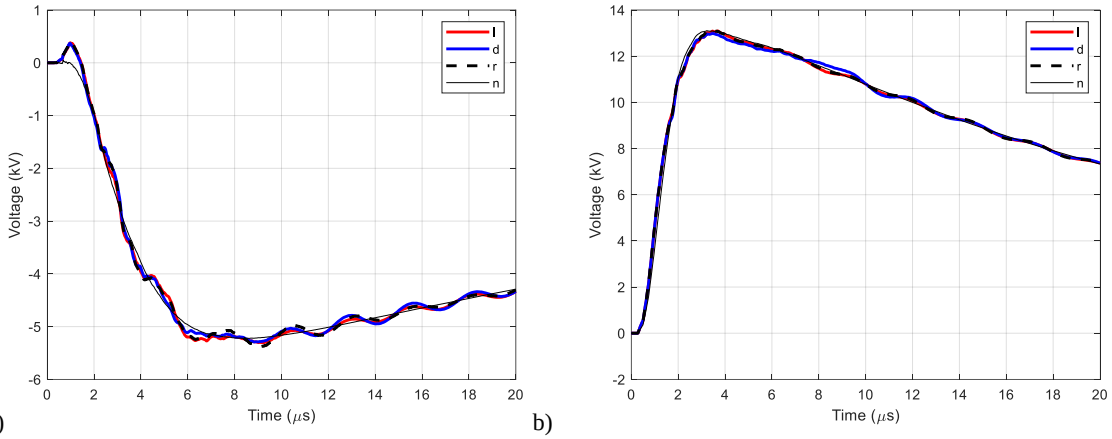

a) b)

Figure 8. Overvoltages induced at the LV transformers terminals by a negative first stroke. a): transformer 1; b): transformer 2.

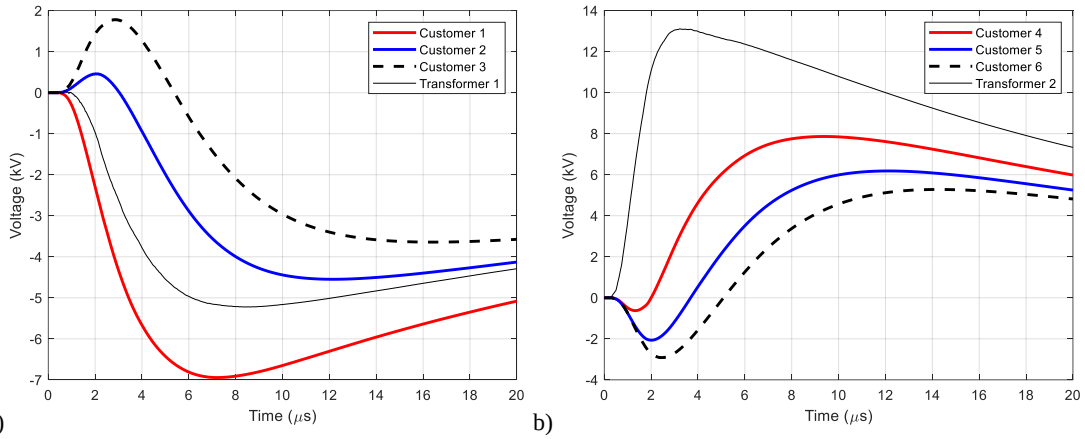

a) b)

Figure 9. Overvoltages in the neutral conductors due to a negative first stroke. a): transformer 1 and customers 1, 2, 3; b): transformer 2 and customers 4, 5, 6.

4. Lightning Performance Results

As mentioned, the estimation of the lightning performance is carried out through the application of the Monte Carlo method. A large number n_{tot} of lightning events is randomly generated. Each event is characterized by the stroke location and the parameters that identify the current waveform at the base of the lightning channel, i.e. the values of the current peak amplitude I_p and equivalent rise time t_f. These two parameters are assumed to follow the Cigré log-normal probability distributions [11, 27] for negative first strokes. As recommended in [11], it is reasonable to expect that the distribution of

the peak amplitude and the front-time duration of the lightning channel-base currents are statistically correlated. The correlation coefficient between the current peak amplitude I_p and equivalent rise time t_f is 0.47. For the calculation of the induced voltages, the current waveform is represented by a trapezoidal function that, as shown in [28], is a good compromise between computational effort and conservative assessment of the lightning performance. For the simulation of direct events, the Cigré waveform is adopted.

The effects of the presence of positive flashes and of subsequent strokes in negative flashes on the lightning performance of the feeder are disregarded.

The stroke locations are assumed to be uniformly distributed in a striking area having a size large enough to include the entire network and all the lightning events that could cause voltages larger than the minimum voltage value of interest for the analysis.

From the total set of n_{tot} lightning events, the ones relevant to indirect lightning are selected by using a lightning incidence model for the line. For this analysis, we have adopted the electro-geometric model proposed in [29].

The results presented in this paper have been obtained with 100000 Monte Carlo events (n_{tot}).

For the case of the double-circuit line with the 69-kV pole configuration, we have considered a 1400 m long line (40 spans of the MV line). The number of indirect events is 96147 and the direct events are 3853. For the case of the MV line alone with the same length, the indirect events are 97100 and the direct events are 2900.

For the case of the double-circuit line with the 138-kV pole configuration, we have considered a 1600 m long line (also in this case 40 spans of the MV line). The indirect events are 96167 and the direct events are 3833.

The lightning performance is expressed by means of a curve providing the expected annual numbers of lightning events F_p that cause voltages with amplitude larger than the insulation voltage value W reported in abscissa:

$$F_p = \frac{n}{n_{tot}} A N_g \tag{7}$$

where n is the number of events causing overvoltages higher than the considered insulation level, A is the striking area (assumed to include all the events at a distance from the line up to 2 km) and N_g is the annual ground flash density (assumed equal to 1 flash/km^2/yr in this paper).

For the calculation of F_p, the flashovers across the insulators are not represented. By including a model of the insulation breakdown, the calculation provides the yearly number of flashovers as presented at the end of this Section.

Figure 10 compares the indirect lightning performance of the MV conductors in the double circuit line (with the 69-kV pole) and the performance of the MV line alone. The figure presents both the total voltages, i.e. the voltages between the line conductor experiencing the largest voltage and the far ground, and the phase to ground voltages, i.e. the voltages between the phase experiencing the largest voltage and the local ground.

Figure 10 shows that the F_p values are significantly lower in the double-circuit configuration with respect to the case of a MV line alone. This is due to the effect of the HV-OGW that provide a shielding effect on the MV circuit and a ground potential rise that reduces the voltage across the insulators (as shown in Figure 3 and Figure 4). The lower F_p values are also due to the lower expected number of indirect events for the case of double-circuit line with respect to the MV line alone. Indeed, for the considered value of N_g, the estimated number of direct events on the OGW is 15.4 flashes/100km/yr, while for the MV line in absence of the HV lines is 11.6 flashes/100km/yr.

Further results concerning the analysis of the lightning performance of the MV line with compact configuration have been presented in [30].

Figure 11 shows the comparison between the lightning performance calculated without SAs and with SAs installed every 280 m in the MV line, which allows a considerable reduction of the F_p values.

Figure 12 shows the lightning performance of the MV line due to direct events to the OGW for the case of R_g = 20 Ω. Due to the peculiar configuration of the line geometry, we assume that shielding failures can be disregarded. The values refer to the voltages across the insulators. A significant improvement of the lightning performance of the considered MV line can be obtained by reducing the spacing between the surge arresters at 140 m.

Figure 13 shows the comparison of the direct lightning performance of the MV line in the double-circuit configuration and alone, assuming in the latter case that all the events hit the messenger. Also for direct strikes, the presence of the HV conductors reduces the F_p values for insulation levels above 120 kV.

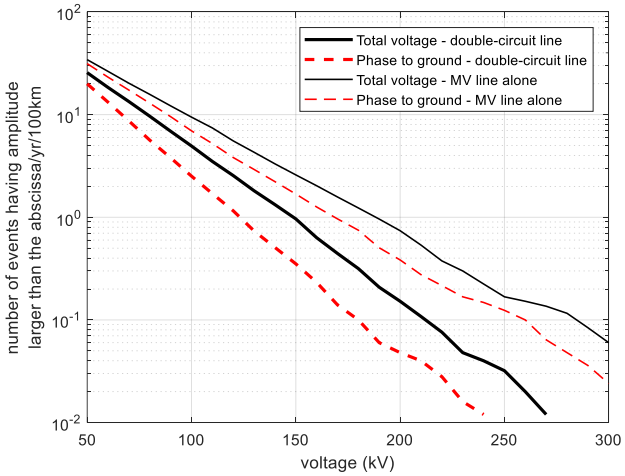

Figure 10. Indirect lightning performance of the MV line in the double-circuit configuration (69-kV pole) and alone. Total voltage in black, voltage respect to M in red. R_g = 20 Ω, σ_g=1mS/m.

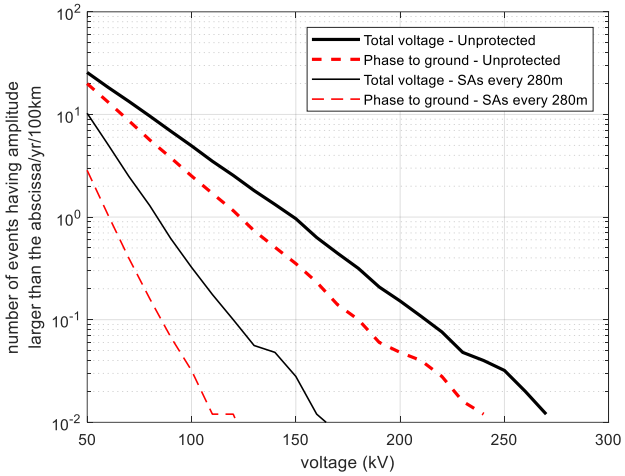

Figure 11. Indirect lightning performance of the MV line in the double-circuit configuration (69-kV) without SAs and with SAs (R_g = 20 Ω, σ_g=1mS/m).

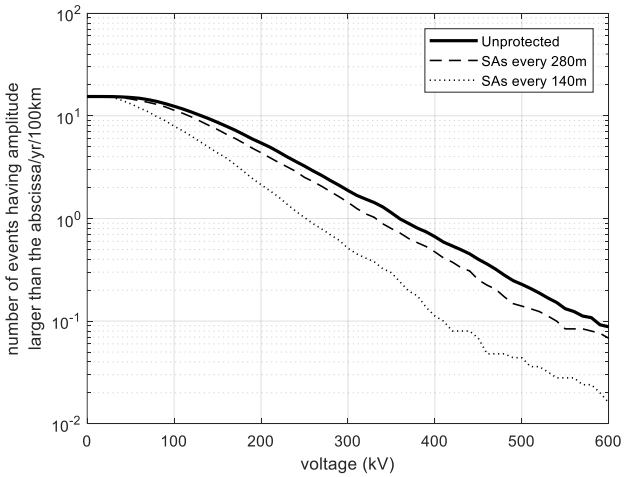

Figure 12. Direct lightning performance (phase-to-ground voltages) of the MV insulators in the double circuit line configuration (69-kV pole) due to direct strikes with and without SAs. R_g = 20 Ω.

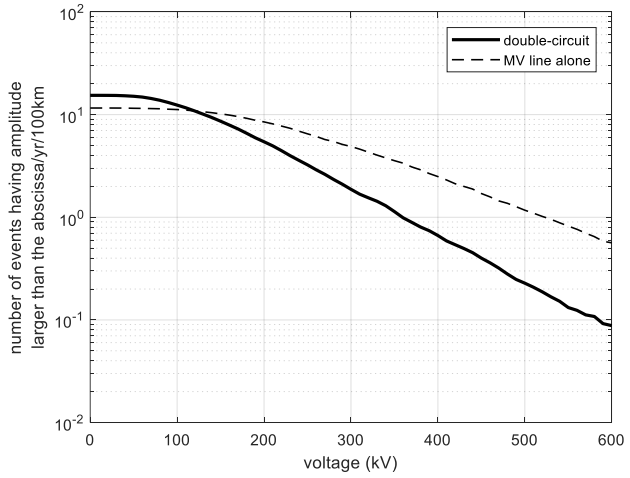

Figure 13. Direct lightning performance (phase-to-ground voltages) of the MV insulators due to direct strikes in the double-circuit line (69-kV pole) and in the MV line alone. R_g = 20 Ω.

Table 4 and Table 5 compare the most relevant results obtained for the 69-kV configuration and for the 138-kV one, respectively. The tables show the F_p values for two different insulation levels (W = 150 kV and 300 kV), for both R_g = 20 Ω and R_g = 40 Ω. The F_p values for the MV line alone (unprotected) are: 10.2 direct events/100 km/yr and 4.9 direct events/100 km/yr for W = 150 kV and W = 300 kV, respectively; 1.7 indirect events/100 km/yr and 0.02 indirect events/100 km/yr for W = 150 kV and W = 300 kV, respectively.

Table 4 and Table 5 also show the reduction of the F_p values obtained by the installation of the SAs.

Table 4. Number of direct (N_d) or indirect (N_i) events/100 km/yr exceeding voltage W in the MV line

69-kV Configuration	W = 150 kV		W = 300 kV	
	N_d	N_i	N_d	N_i
Unprotected (R_g = 20 Ω)	8.6	0.4	1.9	$< 10^{-2}$
SAs every 8 poles (R_g = 20 Ω)	7.4	$< 10^{-2}$	1.4	$< 10^{-2}$
SAs every 4 poles (R_g = 20 Ω)	4.4	$< 10^{-2}$	0.5	$< 10^{-2}$
Unprotected (R_g = 40 Ω)	11.7	0.2	4.2	$< 10^{-2}$
SAs every 8 poles (R_g = 40 Ω)	9.8	$< 10^{-2}$	2.8	$< 10^{-2}$
SAs every 4 poles (R_g = 40 Ω)	5.1	$< 10^{-2}$	0.8	$< 10^{-2}$

Table 5. Number of direct (N_d) or indirect (N_i) events/100 km/yr exceeding voltage W in the MV line

138-kV Configuration	W = 150 kV		W = 300 kV	
	N_d	N_i	N_d	N_i
Unprotected (R_g = 20 Ω)	7.6	0.3	1.4	$< 10^{-2}$
SAs every 8 poles (R_g = 20 Ω)	6.3	$< 10^{-2}$	1.0	$< 10^{-2}$
SAs every 4 poles (R_g = 20 Ω)	3.6	$< 10^{-2}$	0.5	$< 10^{-2}$
Unprotected (R_g = 40 Ω)	11.0	0.2	2.8	$< 10^{-2}$
SAs every 8 poles (R_g = 40 Ω)	8.0	$< 10^{-2}$	1.7	$< 10^{-2}$
SAs every 4 poles (R_g = 40 Ω)	4.2	$< 10^{-2}$	0.6	$< 10^{-2}$

Table 6 compares the number of flashovers per 100 km per year for the case in which the MV line is composed by covered conductors or by bare conductors. The calculation of the flashovers is carried out by using the insulation breakdown model parameters of Table 1.

As expected, for both the considered pole configurations (69-kV and 138-kV), a reduction of the grounding resistance decreases considerably the number of expected flashovers. The adoption of covered conductors further reduces the number of flashovers in the MV line.

Table 6 also shows the number of flashovers for the HV line. The number of flashovers of the 138-kV HV insulators is lower than the one of the 69-kV configuration thanks to the presence of the UGW. The presence of the UGW also decreases the number of flashovers in the MV line of the 138-kV double-circuit configuration with respect to the MV line of the 69-kV configuration.

Table 6. Expected number of flashovers per 100 km/yr due to direct events to OGW

configuration	MV *bare conductors*		MV *covered conductors*		HV	
	R_g = 20 Ω	R_g = 40 Ω	R_g = 20 Ω	R_g = 40 Ω	R_g = 20 Ω	R_g = 40 Ω
69-kV	1.6	4.0	0.3	1.1	0.8	1.5
138-kV	0.8	2.4	0.1	0.5	0.3	0.6

Figure 14-Figure 17 compare the lightning performance of the MV line in case the HV conductors are present or not, for the four different configurations: 69 kV and R_g = 20 Ω (Figure 14), 138 kV and R_g = 20 Ω (Figure 15), 69 kV and R_g = 40 Ω (Figure 16), 138 kV and R_g = 40 Ω (Figure 17). In these figures both direct and indirect events are considered

for the calculation of the lightning performances. As anticipated, the overall lightning performance of the MV line of the multi-circuit configuration is improved with respect to the case of a MV line alone.

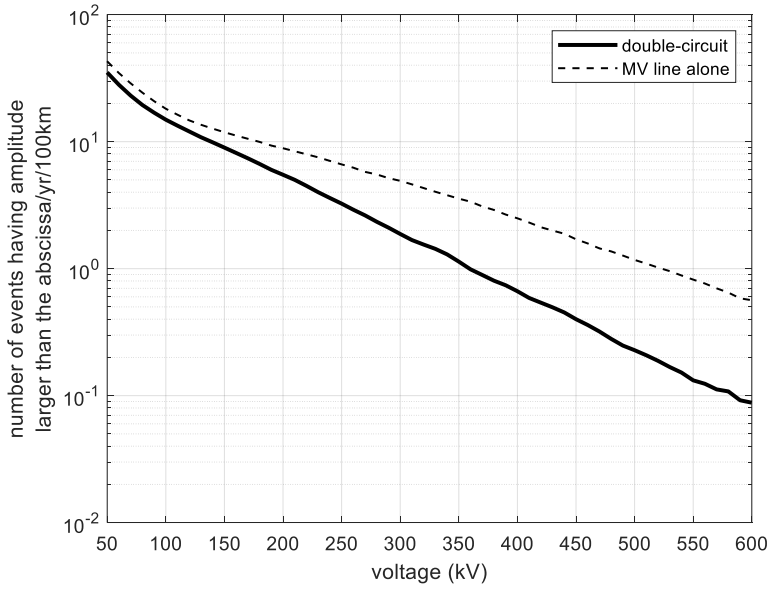

Figure 14. Lightning performance of the 69-kV configuration considering both direct and indirect events. R_g =20Ω

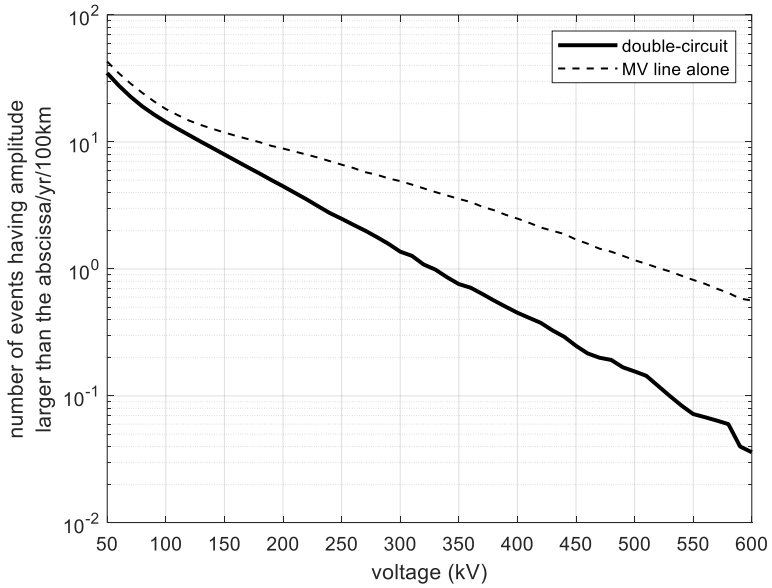

Figure 15. Lightning performance of the 138-kV configuration considering both direct and indirect events. R_g =20Ω

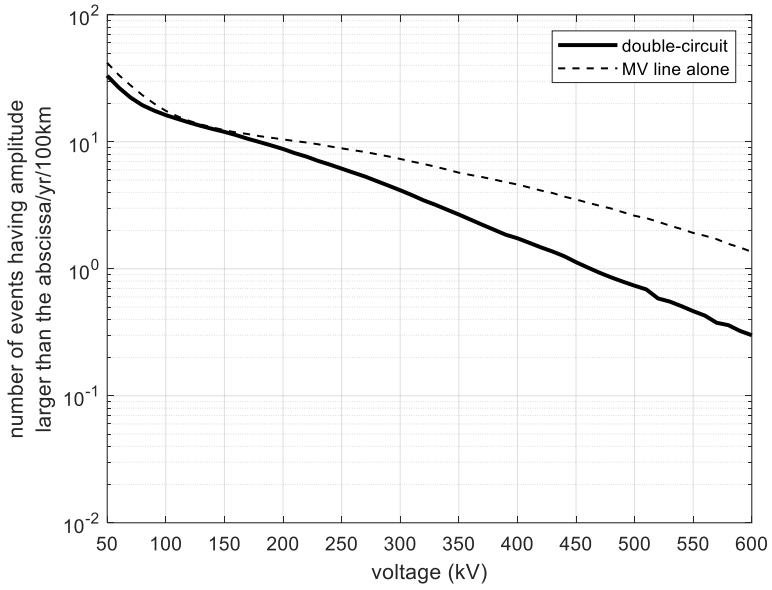

Figure 16. Lightning performance of the 69-kV configuration considering both direct and indirect events. R_g=40Ω

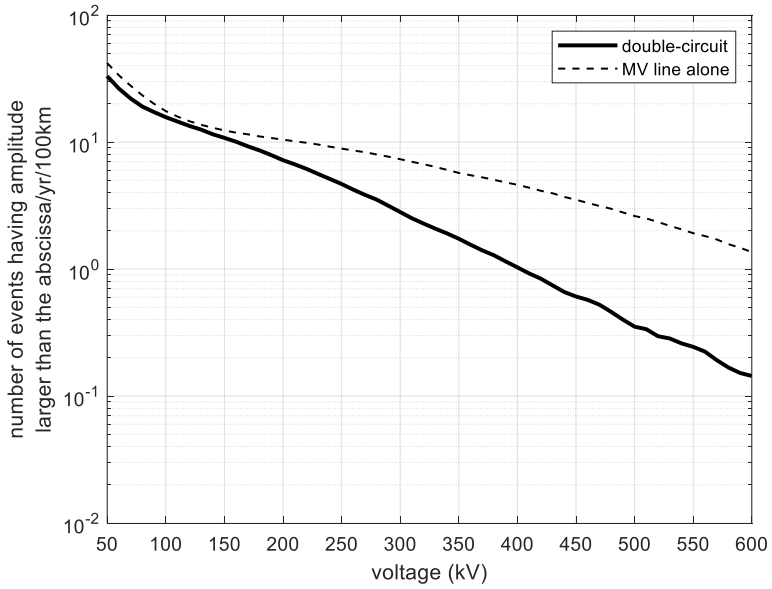

Figure 17. Lightning performance of the 138-kV configuration considering both direct and indirect events. R_g=40Ω

Conclusions

For the double-circuit configurations dealt with in this paper, the compact MV line in the double-circuit line shows a better lightning performance than the MV line alone. The main reasons are:

- although the number of direct strikes increases in the double-circuit configurations

with respect to the MV line alone, the HV grounded wires are effective in limiting the voltage stress of the MV line;

- the voltage induced in the overhead ground wire is larger than in the messenger, causing a significant ground potential rise that reduces the voltage across MV spacers and insulators.

The above applies for the assumed values of grounding resistance, namely 20 Ω and 40 Ω, but it is reasonable to expect that this conclusion would not change substantially for other values of such a parameter, within its typical range.

Through the analysis presented in the paper we have quantified the extent to which the lightning performance of the MV line depends on the line withstand voltage, the grounding resistance and the number of surge arresters.

In case of distribution transformers connected at some MV posts of the distribution line, the neutral conductor of the various customers can experience very high induced voltages respect to the undisturbed grounding. This represents an important aspect that should be taken into account in areas with high ground flash density.

Acknowledgments

This work was developed within the scope of the R&D Program of the Brazilian Electric Energy Sector regulated by ANEEL. Project PD-5217-1515/2015 "Compartilhamento de Estruturas de Linhas de Subtransmissão 72.5 e 145 kV e Redes de Distribuição 15, 25 e 36.2 kV - Estudos Mecânicos, de Transitórios e Modelos para Validação Técnica e Econômica", financed by ENERGISA power company.

5. References

[1] L. Moraes, G. Lopes, A. Violin, A. Piantini, G. Ferraz, J. Campos, R. Salustiano, R. Capelini, E. Wanderley Neto, Assessment of the electromagnetic coupling between lines of different voltages sharing the same structures, CIRED - Open Access Proc. J. 2017 (2017) 531–534. doi:10.1049/oap-cired.2017.1297.

[2] N. Rugthaicharoencheep, W. Thansiphraserth, A. Phayomhom, Comparison voltage across insulator strings of 69 kV and 24 kV lines due to lightning strokes to top pole and mid span, in: 2012 47th Int. Univ. Power Eng. Conf., London, UK, 2012. doi:10.1109/UPEC.2012.6398426.

[3] A. Borghetti, G.M. Ferraz, F. Napolitano, C.A. Nucci, A. Piantini, F. Tossani, Lightning protection of a compact MV power line sharing the same poles of a HV line, in: 34th Int. Conf. Light. Prot. ICLP 2018, IEEE, Rzeszow, Poland, 2018: pp. 1–7. doi:10.1109/ICLP.2018.8503292.

[4] F. Napolitano, A. Borghetti, C.A. Nucci, M. Paolone, F. Rachidi, J. Mahseredjian, An advanced interface between the LIOV code and the EMTP-RV, in: Proc. 29th Int. Conf. Light. Prot., Uppsala, Sweden, 2008: pp. 1–12.

[5] C.A. Nucci, F. Rachidi, Interaction of electromagnetic fields generated by lightning with overhead electrical networks, in: V. Cooray (Ed.), Light. Flash. 2nd Ed., IET - Power and Energy Series 69, London, UK, 2014: pp. 559–610.

[6] A. Borghetti, C.A. Nucci, M. Paolone, An improved procedure for the assessment of overhead line indirect lightning performance and its comparison with the IEEE Std. 1410 method, IEEE Trans. Power Deliv. 22 (2007) 684–692.

doi:10.1109/TPWRD.2006.881463.

[7] A. Borghetti, C.A. Nucci, M. Paolone, Indirect-lightning performance of overhead distribution networks with complex topology, IEEE Trans. Power Deliv. 24 (2009) 2206–2213. doi:10.1109/TPWRD.2009.2021038.

[8] W.A. Chisholm, J.G. Anderson, A. Phillips, J. Chan, Lightning Performance of Compact Lines, in: Proc. X Int. Symp. Light. Prot., Curitiba, Brazil, 2009.

[9] K. Nakada, H. Sugimoto, S. Yokoyama, Experimental facility for investigation of lightning performance of distribution lines, IEEE Trans. Power Deliv. 18 (2003) 253–257. doi:10.1109/TPWRD.2002.803844.

[10] A. Ametani, T. Kawamura, A method of a lightning surge analysis recommended in Japan using EMTP, IEEE Trans. Power Deliv. 20 (2005) 867–875. doi:10.1109/TPWRD.2004.839183.

[11] Cigré Working Group 33.01, Guide to procedures for estimating the lightning performance of transmission lines (TB 63), CIGRE, Paris, 1991.

[12] M. Darveniza, A.E. Vlastos, The generalized integration method for predicting impulse volt-time characteristics for non-standard wave shapes-a theoretical basis, IEEE Trans. Electr. Insul. 23 (1988) 373–381. doi:10.1109/14.2377.

[13] W.A. Chisholm, New challenges in lightning impulse flashover modeling of air gaps and insulators, IEEE Electr. Insul. Mag. 26 (2010) 14–25. doi:10.1109/MEI.2010.5482551.

[14] A.R. Hileman, Insulation Coordination for Power Systems, Marcel Dekker, Inc., New York, 1999.

[15] J.B. Wareing, Covered Conductor Systems for Distribution (EA report), 2005.

[16] R.E. De Souza, R.M. Gomes, G.S. Lima, F.H. Silveira, A. De Conti, S. Visacro,

Preliminary analysis of the impulse breakdown characteristics of XLPE-covered cables used in compact distribution lines, in: 2016 33rd Int. Conf. Light. Prot. ICLP 2016, 2016. doi:10.1109/ICLP.2016.7791387.

[17] A. Borghetti, A.S. Morched, F. Napolitano, C.A. Nucci, M. Paolone, Lightning-induced overvoltages transferred through distribution power transformers, IEEE Trans. Power Deliv. 24 (2009) 360–372. doi:10.1109/TPWRD.2008.2002674.

[18] F. Napolitano, F. Tossani, A. Borghetti, C.A. Nucci, M.L.B. Martinez, G.P. Lopes, G.J.G. Dos Santos, D.R. Fagundes, Lightning performance of a real distribution network with focus on transformer protection, Electr. Power Syst. Res. 139 (2016) 60–67. doi:10.1016/j.epsr.2015.11.019.

[19] F. Tossani, A. Borghetti, F. Napolitano, A. Piantini, C.A. Nucci, Lightning Performance of Overhead Power Distribution Lines in Urban Areas, IEEE Trans. Power Deliv. 33 (2018) 581–588. doi:10.1109/TPWRD.2017.2658183.

[20] F. Tossani, F. Napolitano, A. Borghetti, C.A. Nucci, G.P. Lopes, M.L.B. Martinez, G.J.G. Dos Santos, Estimation of the influence of direct strokes on the lightning performance of overhead distribution lines, in: 2015 IEEE Eindhoven PowerTech, PowerTech 2015, 2015. doi:10.1109/PTC.2015.7232682.

[21] F. Rachidi, C.A. Nucci, M. Ianoz, Transient analysis of multiconductor lines above a lossy ground, IEEE Trans. Power Deliv. 14 (1999) 294–302. doi:10.1109/61.736741.

[22] F. Tossani, F. Napolitano, F. Rachidi, C.A. Nucci, An Improved Approach for the Calculation of the Transient Ground Resistance Matrix of Multiconductor Lines, IEEE Trans. Power Deliv. 31 (2016) 1142–1149. doi:10.1109/TPWRD.2015.2500341.

[23] K. Berger, R.B. Anderson, H. Kroninger, Parameters of lightning flashes, Electra. 41 (1975) 23–37.

[24] F. Heidler, Analytische blitzstromfunktion zur LEMP-berechnung, in: Proc. 18th Int. Conf. Light. Prot., Munich, Germany, 1985: pp. 63–66.

[25] C.A. Nucci, F. Rachidi, M. V. Michel, C. Mazzetti, Lightning-Induced Voltages on Overhead Lines, IEEE Trans. Electromagn. Compat. 35 (1993) 75–86. doi:10.1109/15.249398.

[26] E.D. Sunde, Earth conduction effects in transmission systems, D. Van Nostrand Company, New York, 1968.

[27] R.B. Anderson, A.J. Eriksson, Lightning parameters for engineering applications, Electra. 69 (1980) 65–102.

[28] A. Borghetti, F. Napolitano, C.A. Nucci, F. Tossani, Influence of the return stroke current waveform on the lightning performance of distribution lines, IEEE Trans. Power Deliv. 32 (2017) 1800–1808. doi:10.1109/TPWRD.2016.2550662.

[29] IEEE Std 1410-2010, IEEE guide for improving the lightning performance of electric power overhead distribution lines, IEEE Std 1410-2010 (Revision IEEE Std 1410-2004). (2011) 1–73. doi:10.1109/IEEESTD.2011.5706451.

[30] F. Napolitano, A. Borghetti, D. Messori, C.A. Nucci, M.L.B. Martinez, G.P. Lopes, J.I.L. Uchôa, Assessment of the Lightning Performance of Compact Overhead Distribution Lines, IEEJ Trans. Power Energy. 133 (2013) 1–7. doi:10.1541/ieejpes.134.1.